Available online at www.sciencedirect.com
ScienceDirect
Surface & Coatings Technology 201 (2006) 2953 – 2959
SURFACE & COATINGS TECHNOLOGY
www.elsevier.com/locate/surfcoat

Corrosion resistance of a Zn–Ni electrodeposited alloy obtained with a controlled electrolyte flow and gelatin additive

M.E. Soares [a], C.A.C. Souza [b], S.E. Kuri [c,*]

[a] Centro Federal de Educação Tecnológica-Pr, Brazil
[b] Departamento de Ciências e Tecnologia dos Materiais, Universidade Federal daBahia, Brazil
[c] Departamento de Engenharia de Materiais, Universidade Federal de São Carlos, Rodovia Washington Luis, km 235, 13565-905-São Carlos/SP, Brazil

Received 21 November 2005; accepted in revised form 7 June 2006
Available online 12 July 2006

Abstract

Studies of the factors that enhance the corrosion resistance of electrodeposited Zn–Ni alloys are highly relevant due to these alloys' widespread industrial use as protective coatings for steel substrates. This paper reports on an investigation into the effect of the flow rate and the addition of gelatin to the plating bath on the corrosion resistance of Zn–Ni electrodeposits. An increase in the flow rate and gelatin content in the plating bath promoted an increase in the corrosion resistance of Zn–Ni deposit. This behavior cannot be explained in terms of composition because it involves the grain morphology of the electrodeposited alloy.

Keywords: Electrodeposition; SEM; Amorphous alloys; Corrosion

1. Introduction

The use of zinc and zinc alloys to improve the corrosion resistance of coated steel sheets has been widely studied due to its importance in industrial contexts. Zn–Ni electrodeposits offer a particularly promising alternative to pure Zn and galvannealed steel, mainly in the automotive industry, due to their improved mechanical properties and corrosion resistance [1,2]. The aeronautical industry has shown increasing interest in Zn–Ni alloy coating as a substitute for toxic and high-cost cadmium coatings [3]. Barcelo et al. [4] reported that alloys containing 10 wt.% to 15 wt.% of Ni displayed superior corrosion resistance. However, the highest Ni content commonly employed in the aeronautical industry is 15 wt.% to 22 wt.%.

The electrodeposition of zinc alloys with iron group metals causes the anomalous phenomenon of codeposition, whereby zinc – the less noble metal – is deposited preferentially. Anomalous codeposition is therefore a very important phenomenon in the electrodeposition of zinc alloys.

Abou-Krish [5] reported that the deposition of Ni requires a low nucleation overpotential, while the deposition of Zn takes place at a higher nucleation potential and Zn–Ni is codeposited at a moderate potential. According to him, this behavior indicates that the deposition of Ni is strongly inhibited by the presence of Zn^{2+}, while the deposition of Zn is induced by the presence of Ni^{2+}. However, Zn–Ni alloy codeposition is not always anomalous. Experimental results for chloride and sulfate solution [6,7] suggest that anomalous codeposition is preceded by normal codeposition, in which hydrogen reduction prevails. In sulfate solution, the normal Zn–Ni codeposition is influenced by mass transport and electrolyte composition, but these factors do not affect anomalous Zn–Ni codeposition [6].

The literature contains reports about the mechanism of anomalous Zn–Ni alloy codeposition. This codeposition was first explained by the hydroxide suppression mechanism [8,9], which is based on the presence of high pH near the cathode and the resulting formation of $Zn(OH)_2$ films. During electrodeposition, water is reduced to H_2 gas and OH ions at the cathode. Since the concentration of interfacial OH ions is increased by this reaction, the pH near the cathode rises, enabling the

* Corresponding author. Tel.: +55 16 33518507; fax: +55 16 33615404.
E-mail addresses: msoares@pg.cefetpr.br (M.E. Soares), caldassouza@hotmail.com (C.A.C. Souza), dsek@power.ufscar.br (S.E. Kuri).

0257-8972/$ - see front matter © 2006 Elsevier B.V. All rights reserved.
doi:10.1016/j.surfcoat.2006.06.006

formation of $Zn(OH)_2$ films on the cathode. These films inhibit the reduction of Ni_2^+ ion, while Zn is reduced in these films, so that the Zn base metal is electrodeposited preferentially onto the cathode. However, it is not clear whether the formation of hydrogen suffices to cause major alkalization effects that allow for the formation of $Zn(OH)_2$ films [10].

In addition to the hydroxide suppression mechanism, anomalous Zn–Ni codeposition is explained by the formation of a mixed intermediate $(NiZn)^+_{ads}$ [11], and by another proposition based on the underpotential deposition of zinc on nickel-rich zinc alloys or on nickel nuclei [12,13].

The literature on the electrodeposition of iron group alloys also contributes shed further light on anomalous Zn–Ni codeposition. Results [14] on Ni–Fe electrodeposition confirmed that Ni deposition is inhibited by the presence of Fe^{2+} ion, and that the Fe deposition rate is enhanced by the presence of Ni^{2+} ions in comparison with single metal deposition. This behavior is coherent with that reported by Abou-Krish [5] for Zn–Ni electrodeposition alloy, and demonstrates that the anomalous codeposition of iron group metals involves both inhibiting and accelerating effects. According to Matlosz [15], the inhibition of the more noble nickel in the presence of iron is caused by preferential surface coverage of the adsorbed iron intermediate, resulting from a difference between the two elements in the Tafel constant for the electrodeposition step. Matlosz proposed that a two-step reaction mechanism involving adsorbed monovalent intermediate ions for the electrodeposition of iron and nickel as single metals can be combined to form a predictive model for the codeposition of iron–nickel alloys. According to Matlosz [15], the results obtained suggest that hydrogen and nickel–iron kinetics are essentially uncoupled and may be treated separately in the development of the alloy deposition process.

Sasaki and Talbot [16] proposed a mechanism of iron-group metal and binary alloy electrodeposition based on Grande and Talbot's one-dimensional diffusion model [17] to determine near-surface concentrations of the ionic species for electrodeposition. Sasaki and Talbot's model [16] expands upon the surface kinetics by including the effects of competitive adsorption, site blockage by hydrogen atoms, and a variance in the number of adsorption sites. According to the authors, the main contribution of this model is the inclusion of hydrogen adsorption and its effect on electrodeposition.

The presence of Zn in Zn–Ni alloys provides cathodic protection of iron-based substrates while Ni increases the deposit's corrosion resistance. The beneficial influence of Ni is that it improves the passive oxide film's protective characteristic [18], and the alloy structure. The higher corrosion resistance of electrodeposited Zn–Ni coatings has been attributed to the predominant presence in the oxide layer of crystallographic planes with a higher packing density and hence a more stable ionization in the environment [19].

The literature reports on investigations into new Zn–Ni alloy electrodeposition techniques, such as compositionally modulated multilayers (CMM) and the use of a duct-shaped electrochemical cell with controlled electrolyte flow, as well as the effect of gelatin, a nontraditional additive, on the characteristics of Zn–Ni alloys. Experimental results [20] have shown that Zn–Ni CMM coatings are more corrosion resistant than monolithic zinc or nickel coatings of similar thickness. The efficiency of the electrodeposition process and the characteristics of the Zn–Ni deposit can be improved by adding additives such as gelatin to the plating bath, and by the use of a duct-shaped electrochemical cell with controlled electrolyte flow [21].

The use of an electrochemical cell in the form of a duct with a controlled electrolyte flow is interesting for the following reasons [22,23]. (a) In the laboratory, this type of cell allows one to simulate flow conditions in industrial electrodeposition systems. (b) Studying the current distribution with a controlled flow allows one to control the thickness and homogeneity of the deposited layer. (c) Electrochemical cells are easy to build. (d) Industrial production volumes can be increased through the sequential use of electrochemical cells. In addition to these advantages, it has been found that the efficiency of Zn–Ni alloy electrodeposition in a tubular cell with laminar electrolyte flow (2 ml/s) is higher than deposition in the stationary state.

However, the literature lacks information about the effect produced by adding gelatin and by the plating bath flow on the corrosion resistance of Zn–Ni deposits. The purpose of this study is to ascertain how the corrosion resistance of Zn–Ni alloy electrodeposited from a duct-shaped electrochemical cell with controlled electrolyte flow is affected by the flux rate and the gelatin concentration.

2. Experimental procedure

The electrodeposition was carried out at 40 °C in an aerated solution in a duct-shaped cell with controlled electrolyte flow, as illustrated schematically in Fig. 1. The flow of electrolyte in the cell was calculated based on the following equation [24]:

$$Re = \frac{Q \cdot \rho}{b \cdot \mu} \tag{1}$$

where Q is the flow of electrolyte, b is the width of the electrochemical cell's square transversal section, ρ is the

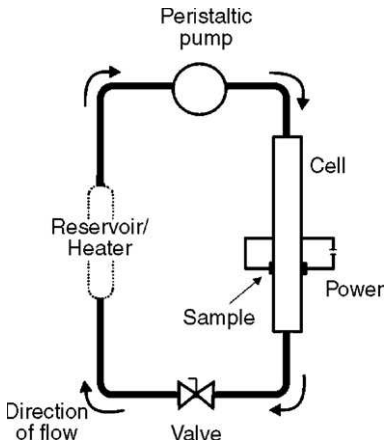

Fig. 1. Schematic representation of the electrodeposition system.

Table 1
Plating bath reagent concentrations and functions [11]

Reagent	Concentration (10^{-3} g/cm^3)	Function
$NiCl_26H_2O$	34.5	Ni source
$ZnCl_2$	38.5	Zn source
NH_4Cl	150.0	Increase electrolytic conductivity
H_3BO_3	20.0	Buffer

specific weight of the plating bath, μ is the plating bath viscosity, and *Re* is Reynold's number.

Depositions were made with different Q values, applying 2.0 ml/s, 7.0 ml/s and 13.0 ml/s flows, which correspond, respectively, to Reynold's numbers of 1200 (laminar flow), 4000 (transitory flow) and 8000 (turbulent flow).

The Zn–Ni alloys were deposited on an AISI 4340 steel disc substrate (1.13 cm^2) from the basic plating bath shown in Table 1. A commercial grade gelatin (a protein with C, N, H and O) was added to the plating bath and the effects of various concentrations were analyzed.

The galvanostatic depositions were carried out at a current density of 10 mA/cm^2 and at a sufficiently high charge density to produce 5 μm thick deposits. This thickness is a typical value in a galvanizing line. Platinum foil was used as a counter electrode.

The thickness of the deposit, L, was calculated using the following equation:

$$L = \frac{m_t}{d_t \cdot A} \tag{2}$$

where m_t is the total mass of the deposit, A is the surface area of substrate, and d_t is the density of deposit, which is obtained from Eq. (3).

$$d_t = d_{Zn} \cdot \frac{m_{Zn}}{m_t} + d_{Ni} \cdot \frac{m_{Ni}}{m_t} \tag{3}$$

In Eq. (3), d_{Zn} represents the densities of Zn, d_{Ni} the densities of Ni, m_{Zn} the amount of Zn in the deposit, and m_{Ni} is the amount of Ni in the deposit.

The parameters for analyzing the corrosion resistance were measured at 25 °C using a SOLARTRON 1287 electrochemical interface. These parameters – polarization resistance (R_p) and corrosion current density (i_{cor}) – were measured using CORRWARE software. To measure the i_{cor}, the linear polarization resistance technique was used. This parameter was obtained as a function of R_p, with b_c as the cathodic and b_a the anodic Tafel constants. An aerated stagnant solution of 0.6 M NaCl was used as an aggressive solution. The three-electrode electrochemical cell was used with a Pt foil counter and saturated calomel electrode (SCE) containing a Lughin capillary as reference electrode. To begin the measurements, the sample was introduced into the cell and was allowed to reach equilibrium, which usually took around 10 min.

The corrosion rate, MPY (expressed in mm per year), was obtained from i_{cor} according to the equation below:

$$\mathrm{MPY} = \frac{k \cdot i_{cor} \cdot W}{d_t \cdot F} \tag{4}$$

where i_{cor} is the corrosion current density determined by the linear polarization method using the Stern-Geary equation [25], F is Faraday's constant, W is the alloy's specific weight obtained from Eq. (5), d_t is the deposit's density obtained from Eq. (3), and k is a constant which depends on the units used.

$$W = \%\mathrm{Zn} \cdot W_{Zn} + \%\mathrm{Ni} \cdot W_{Ni} \tag{5}$$

where W_{Zn} is the Zn atomic weight, W_{Ni} is the Ni atomic weight, %Zn is the percent of Zn in the deposit, and %Ni is the percent of Ni in the deposit.

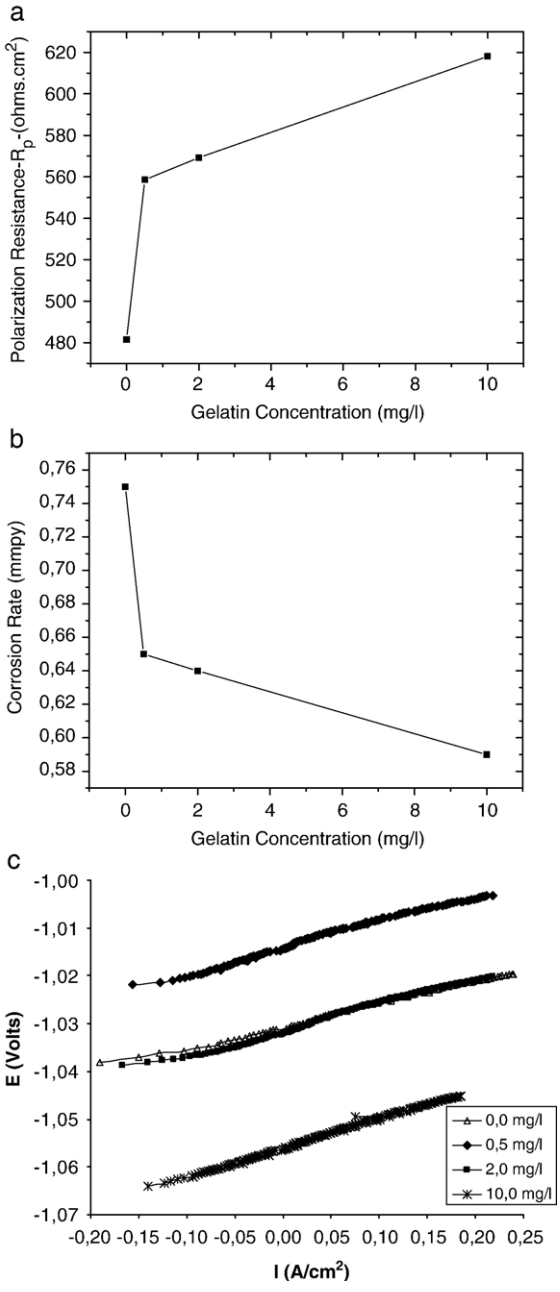

Fig. 2. Corrosion parameters of Zn–Ni electrodeposits in 0.6 M NaCl solution obtained from plating bath containing several concentrations of gelatin in a laminar flow (2 ml/s). (a) Polarization resistance, R_p, (b) corrosion rate, MPY (expressed in mm per year); and (c) polarization curves around open circuit potential used to measure R_p as a function of gelatin concentration.

The composition of the electrodeposited alloy was determined by energy dispersive X-ray spectroscopy (EDS), performed in a Carl Zeiss model DSM 940 A scanning electron microscope (SEM) equipped with an energy dispersive X-ray analyzer.

3. Results and discussion

An investigation was made of how the flow and the gelatin content in the plating bath affected the corrosion resistance of Zn–Ni deposit on the steel AISI 4340 substrate. Fig. 2a shows the results corresponding to the influence of gelatin additive on the R_p values in a constant laminar flow of 2 ml/s, while Fig. 2b shows the corresponding corrosion rate, MPY (expressed in mm per year). Fig. 2c shows, as an example, the polarization curves used for R_p corrosion measurements as a function of the gelatin concentration.

Fig. 3a indicates the influence of the flow rate on the R_p values, considering a constant gelatin concentration of 2 mg/l, while Fig. 3b shows the corresponding corrosion rate. Prior results have shown that the presence of this gelatin content increases the efficiency of the deposition process, although higher concentrations do not significantly enhance the deposition efficiency [21].

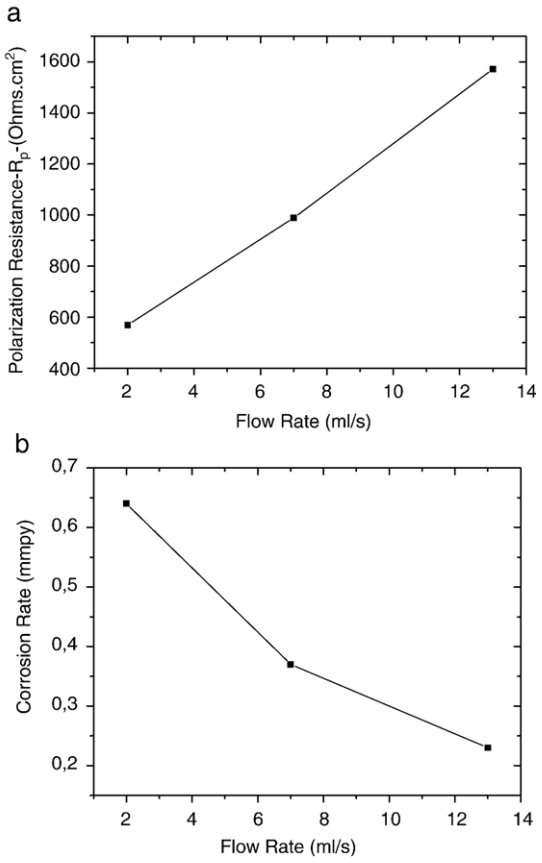

Fig. 3. Corrosion parameters of Zn–Ni electrodeposits in 0.6 M NaCl solution, obtained from plating bath containing 2 ml/l of gelatin and several flow rates. (a) Polarization resistance, R_p, and (b) corrosion rate, MPY (expressed in mm per year).

Table 2
Effect of gelatin concentration on the Zn–Ni deposits composition obtained from bath deposition at 2.0 ml/s

Gelatin concentration (mg/l)	0.0	0.5	2	10
%Ni	11.6	13.5	11.5	9.8

As indicated in Fig. 2, an increase in gelatin content led to a significant increase in R_p and a consequent decrease in the corrosion rate. The same behavior occurred when the electrolyte flow rate was increased, as illustrated in Fig. 3a and b. These results therefore indicate enhancement of the deposit's corrosion resistance with the addition of gelatin and with the increased plating bath flow rate.

The polarization resistance and corrosion rate of AISI 4340 steel obtained in the aerated stagnant 0.6 M NaCl solution were 1330 Ω and 0.27 MPY (expressed in mm per year), respectively. The results depicted in Figs. 2 and 3 indicate that, except for the deposits obtained in a bath with 2 mg/l of gelatin and a flow rate of 13 ml/s, all the deposits presented a higher corrosion rate than that of AISI 4340 steel substrate. This means that all the coatings acted as sacrificial anodes. However, the deposit obtained from a plating bath content of 2.0 mg/l and a flux rate of 13.0 ml/s presented a higher corrosion resistance than the steel, indicating that this deposit is inadequate for the cathodic protection of AISI 4340 steel substrate.

The effect of the gelatin concentration and electrolyte flow rate on the composition and morphology of deposits was analyzed in order to understand the behavior of deposits in terms of corrosion resistance. Table 2 shows the effect of gelatin on the nickel concentration in the electrodeposits, considering a flow rate of 2.0 ml/s. Similarly, Table 3 shows the effect of the flow rate on the nickel concentration. Fig. 4 indicates the structures of different deposits as a function of gelatin content at a constant flow rate (2 ml/s), while Fig. 5 shows the effect of the flow rate with a constant gelatin content of 2.0 mg/l. As can be seen, the morphology of the deposit is highly dependent on the gelatin concentration and the flow rate. Hence, the deposit's corrosion resistance is closely correlated to its morphology and composition.

The addition of Ni in Zn–Ni alloys increases the deposit's corrosion resistance [18]. However, the results in Table 2 reveal that, except in the presence of 0.5 mg/l of gelatin, an increase in the bath's gelatin concentration does not ensure an increase in the deposit's nickel content. Similarly, an increase in the bath's flow rate does not increase the Ni content in the deposit. Nevertheless, increasing both gelatin content and flow rate enhances the corrosion resistance of deposits, as indicated in

Table 3
Effect of flow rate on the Zn–Ni deposits composition obtained from bath deposition content 2.0 mg/l of gelatin

Flow rate (ml/s)	2.0	7.0	13.0
%Ni	12.0	12.5	10.4

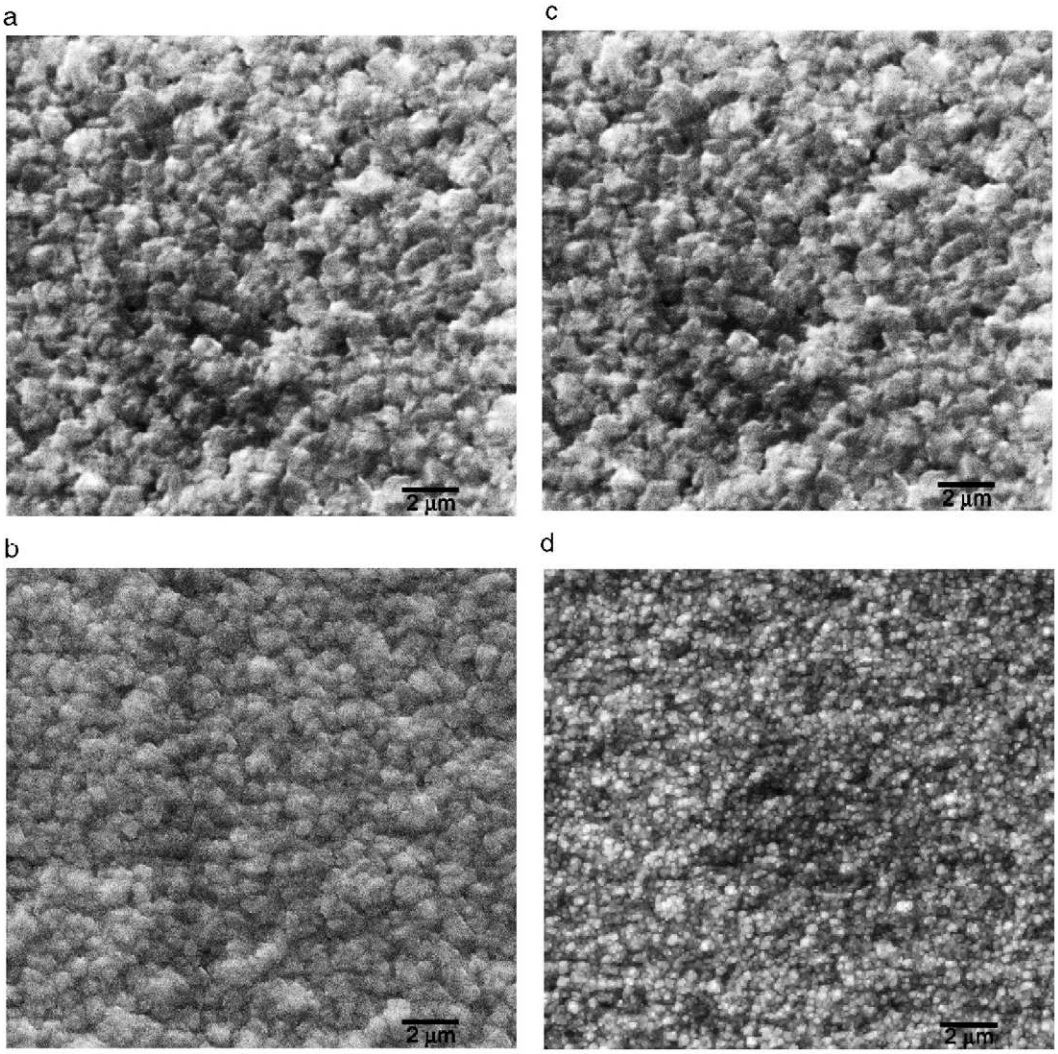

Fig. 4. SEM micrographs of Zn–Ni deposit obtained from plating bath with a 2.0 ml/s flow and several concentrations of gelatin: (a) 0.0 mg/l of gelatin; (b) 0.5 mg/l of gelatin; (c) 2.0 mg/l of gelatin; (d) 10.0 mg/l of gelatin.

Figs. 2 and 3. Our results also indicate that the Ni content in the deposits decreased in the turbulent flow (13 ml/s) and in the bath containing 10 ml/g of gelatin. Therefore, with regard to the flow rate and the addition of gelatin in the plating bath, our results indicate that the corrosion resistance is more strongly affected by the deposit's structure than by its composition.

Fig. 4 indicates that, at a 2 ml/s flow, the presence of 10 mg/l of gelatin diminished the grain size. This grain refinement and the greater compactness of the deposit may be attributed to the higher corrosion resistance of the deposit containing 10 mg/l of gelatin additive. These results are congruent with those obtained by Pagotto et al. [26], who reported that the grain refinement of Zn–Ni alloy achieved though pulsed electrodeposition resulted in a higher corrosion resistance than that of deposits produced by continuous electrodeposition.

Smaller grain sizes mean higher density of defects (mainly grain boundary), so higher corrosion rates are to be expected. However, the augmented corrosion resistance of Zn–Ni electrodeposits in response to grain refinement may be attributable to the enhanced protective performance of the passive film. The formation of oxide film on the corroded surface is diffusion controlled, and it is possible that the greater grain boundary area aids the diffusion of elements toward the surface, thus leading to the formation of a more protective film. This assumption is underpinned by reports that the diffusion of elements in nanocrystalline materials is much higher than in polycrystalline materials [27] and by Youssef et al.'s results [28]. These authors, who analyzed the zinc electrodeposited in a 0.5 N NaOH solution, stated that the decrease in grain size resulted in an improvement of the passive film's protective performance, thus increasing the corrosion resistance.

However, an analysis of Fig. 4a, b and c indicates that grain refinement did not occur in response to the addition of 0.5 mg/l and 2 mg/l of gelatin. Therefore, grain refinement alone does not suffice to explain the results obtained, which strongly suggests the existence of other effects.

The Fig. 5 series indicates that an increase of mass transfer in response to a higher flow rate may play an important role in the microstructure. These figures show that an increase in the flow rate promotes axial grain formation. Fig. 5c, which corresponds

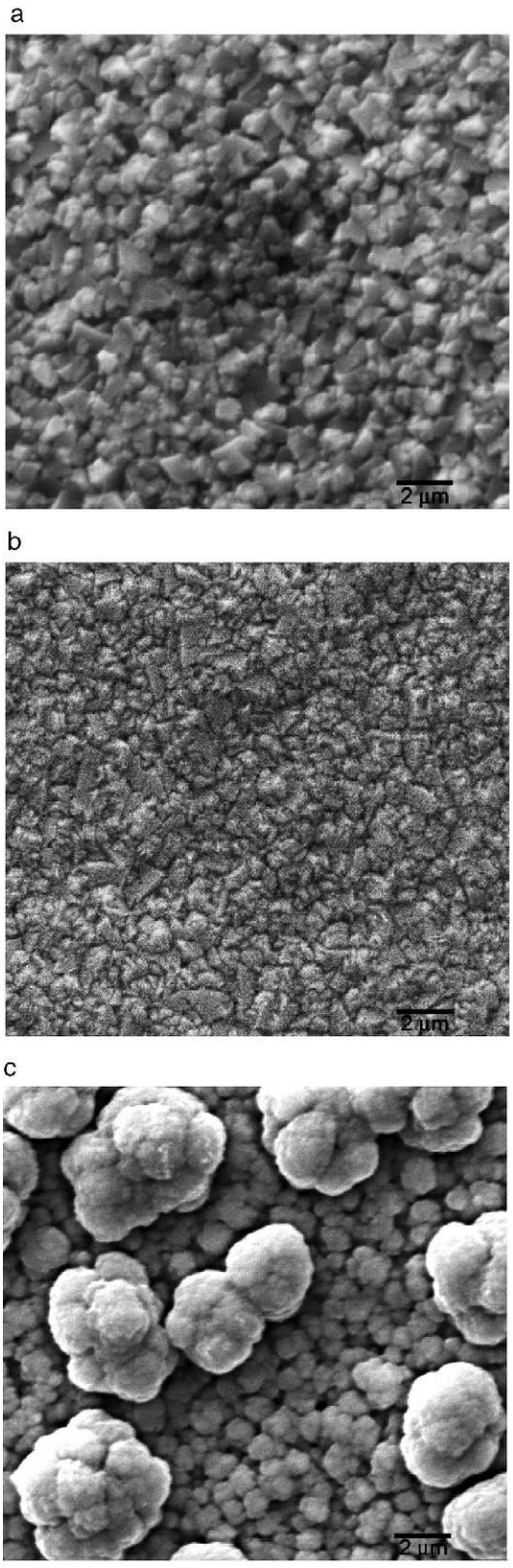

Fig. 5. SEM micrographs of Zn–Ni deposit obtained from solution content of 2.0 mg/l of gelatin and several flow rates: (a) 2.0 ml/s; (b) 7.0 ml/s; and (c) 13.0 ml/s.

to turbulent flux (10 ml/s), reveals the presence of white grains, probably indicating the presence of new nucleation sites in the layer before deposition (gray grains). However, an in-depth investigation of the crystal size is still ongoing. The appearance of this new layer may have resulted from the higher mass transfer caused by the increased flow rate. This assumption is coherent with prior results [21] reporting on a higher deposition efficiency associated with the presence of this second deposit layer. It is possible that higher flow rates aid the diffusion of elements such as oxygen in Zn–Ni deposits and hence the possible formation of a more protective oxide film, which enhances the corrosion resistance. However, the possible presence of a passive film and its composition still requires further study.

The micrograph in Fig. 4d also reveals the presence of white grains, indicating that the addition of gelatin can aid the mass transfer and thus enhance the deposit's corrosion resistance.

The effect of the addition of gelatin and the plating bath flow rate on the corrosion of Zn–Ni deposits may also be related with increased compressive stresses in the deposits. Compressive strains on the surface are known to reduce the corrosion rate when compared with tensile stresses. Mishra and Balasubramaniam [29] analyzed Ni electrodeposits and reported that the magnitude of compressive strain with pulsing was higher than with direct current deposition, and also higher when saccharine was added than without the addition of this addictive. In this study we did not estimate the microstrain, but its effect on added gelatin and on the flow rate will be investigated in future studies.

4. Conclusions

The increase in the plating bath flow from laminar (2.0 ml/s) to transitory (7.0 ml/s) and to turbulent (13.0 ml/s) enhanced the corrosion resistance of Zn–Ni deposit.

An increase of gelatin content in the plating bath promoted an increase in corrosion resistance of the Zn–Ni deposit.

Since the Ni content in the Zn–Ni deposits did not increase with the gelatin content and the plating bath flow rate, the presence of this element does not explain the effect of these factors on the corrosion resistance of Zn–Ni deposits. Because of its strong dependence on the microstructure, the Ni content in the deposits offered insufficient information to allow us to reach a conclusion regarding the corrosion resistance.

References

[1] N.R. Short, S. Zhou, J.K. Dnnis, Surf. Coat. Technol. 79 (1996) 218.
[2] R. Ramanauskas, Appl. Surf. Sci. 153 (1999) 53.
[3] A.M. Alfantazi, J. Page, U. Urb, J. Appl. Electrochem. 26 (1996) 1225.
[4] G. Barcelo, E. Garcia, M. Sarret, C. Muller, J. Appl. Electrochem. 28 (1998) 1113.
[5] M.M. Abou-Krish, Appl. Surf. Sci. 252 (2005) 1035.
[6] F.J. Fabri Miranda, O.E. Barcia, S.L. Diaz, O.R. Mattos, R. Wiart, Electrochim. Acta 41 (1996) 1041.
[7] E. Hall, Plating Surf. Finish. 70 (1983) 59.
[8] H. Dahms, I.M. Croll, J. Electrochem. Soc. 112 (1965) 771.
[9] D.E. Hal, Plating Surf. Finish. 70 (1983) 59.
[10] J. Horans, J. Electrochem. Soc. 128 (1981) 45.

[11] I. Chassang, R. Wiart, Electrochim. Acta 37 (1992) 545.
[12] M.J. Nicol, H.I. Philip, J. Electroanal. Chem. 70 (1976) 233.
[13] S. Swathirajan, J. Electrochem. Soc. 133 (1986) 671.
[14] N. Zech, E.J. Podhaha, D. Landolt, J. Electrochem. Soc. 146 (1999) 2886.
[15] M. Matlosz, J. Electrochem. Soc. 140 (1993) 2272.
[16] K.Y. Sasaki, J.B. Talbot, J. Electrochem. Soc. 147 (2000) 189.
[17] W.C. Grande, J.B. Talbot, J. Electrochem. Soc. 140 (1993) 675.
[18] J.R. Vilche, K. Juttner, W.J. Lorenz, W. Kautek, W. Paatsch, M.M. Dean, U. Stemming, J. Electrochem. Soc. 136 (1989) 3773.
[19] R. Ramanauskas, P. Quintana, L. Maldonado, R. Pomés, M.A. Pech-Canul, Surf. Coat. Technol. 92 (1997) 16.
[20] J. Fei, G.D. Wilcox, Surf. Coat. Technol. 200 (2006) 3533.
[21] M.E. Soares, C.A.C. Souza', S.E. Kuri, Mater. Sci. Eng., A 402 (2005) 16.
[22] Y.S. Jin, Surf. Coat. Technol. 106 (1998) 220.
[23] R. Winand, J. Appl. Electrochem. 21 (1991) 377.
[24] M. FOX, Mechanical Fluids, 5th editionEditora Moderna, Rio de Janeiro, 1984.
[25] M. Stearn, L. Geary, J. Electrochem. Soc. 104 (1957) 56.
[26] S.O. Pagotto Jr., C.M.A. Freire, M. Ballester, Surf. Coat. Technol. 122 (1999) 10.
[27] R. Wurschum, U. Brosmann, H. Shaefer, Diffusion in nanocrystalline materials, in: C.C. Koch (Ed.), Nanostructured Materials: Processing, Properties, and Applications, Noyes Publications, New York, 2002.
[28] Kh.M.S. Youssef, C.C. Koch, P.S. Fedkiw, Corros. Sci. 46 (2004) 51.
[29] R. Mishra, R. Balasubramaniam, Corros. Sci. 46 (2004) 3019.